Journal Pre-proof

Thermally stimulated color-tunable performance of $Ca_3Ga_4O_9$: Bi^{3+} by co-doping with alkali metal ions

Lihong Yin, Yafang Wang, Dirk Poelman, Peter D Townsend

PII: S0925-8388(24)02982-7

DOI: https://doi.org/10.1016/j.jallcom.2024.176395

Reference: JALCOM176395

To appear in: *Journal of Alloys and Compounds*

Received date: 5 June 2024
Revised date: 25 August 2024
Accepted date: 6 September 2024

Please cite this article as: Lihong Yin, Yafang Wang, Dirk Poelman and Peter D Townsend, Thermally stimulated color-tunable performance of $Ca_3Ga_4O_9$: Bi^{3+} by co-doping with alkali metal ions, *Journal of Alloys and Compounds,* (2024) doi:https://doi.org/10.1016/j.jallcom.2024.176395

Thermally stimulated color-tunable performance of $Ca_3Ga_4O_9$: Bi^{3+} by co-doping with alkali metal ions

Lihong Yin [a, b], Yafang Wang [a, *], Dirk Poelman [b] and Peter D Townsend [c]

[a] School of Science, China University of Geosciences, Beijing, 100083, China

[b] LumiLab, Dept. Solid State Sciences, Ghent University, Ghent, 9000, Belgium

[c] School of Science, University of Sussex Brighton, BN1 9QH, UK

* Corresponding author.

E-mail address: wyfemail@gmail.com

Abstract: Thermally stimulated color-tunable persistent luminescent materials can serve in many practical applications. Integrating color-tunable luminescence into a stable charge carrier trapping phosphor is a promising strategy but remains a challenge. In this work, by co-doping with alkali metal ions, $Ca_{2.90}Ga_4O_9$: 5 mol% Bi^{3+}, 5mol% A^+ (A^+= Li^+, Na^+, K^+) phosphors show noticeable thermal stimulated luminescence color-tunability. Among these samples, the phosphor co-doped with Na^+ shows a dramatic color variation with temperature from cyan (513 nm) at 99 ºC to yellow (602 nm) at 237 °C. Further studies confirm that the thermally stimulated color-tunable feature of sample is attributed to the interplay between dual-traps and different emission centers. This work reports the dynamic color-tunable persistent luminescence under different temperatures in alkali metal ions co-doped gallate and provides a new perspective for the design of thermally responsive dynamic optical materials for the application of visual temperature warning or counterfeiting.

Keywords: thermally stimulated color-tunability, $Ca_3Ga_4O_9$: Bi^{3+}, alkali metal ions

1. Introduction

Charge carrier trapping phosphors are defined as a kind of energy storage type luminescence material, which could store energy under the excitation of UV light, X-rays, etc, and then release energy to produce light through photon emission after the excitation light has been switched off. For charge carrier trapping phosphors, it is generally believed that the intrinsic defect sites or traps related to intentional co-dopants are the main causes, because the trap depth is an important factor for the design of long persistent or optically stimulated luminescence (OSL) and thermoluminescence (TSL) materials. The long persistent luminescence phenomenon is attributed to the recombination of charge carriers that are slowly excited by thermal stimulation at room temperature (shallow traps) [1], OSL and TSL also allow to empty deep traps. In the latter case, near-infrared light and thermal stimulation can be used to release the prestored energy by charge carrier de-trapping processes [2-4].

Benefitting from this unique property, charge carrier trapping phosphors have attracted great attention due to the great application of prospect in the field of anti-counterfeiting [5,6], optical information storage [7,8], and radiation dosimeters [9-15]. However, due to the limitation of monochromatic emission of traditional luminescent materials, it is not straightforward to use them in practical applications such as industrial temperature detection and high-security level anti-counterfeiting technology [16-18]. The conventional technique to obtain tunable multi-color properties is modulating the host-activators composition [19-22], hereby only allowing multicolor in different samples, another strategy is to adjust the excitation wavelength, but this steady state PL can be easily counterfeited by substitutes [23]. So realizing dynamic multicolor even under a fixed stimulus in a single host material remains a challenge.

Recent developments in dynamic color-tunable luminescent materials introduce some different methods for authentication based on emission colors. Relying on the energy transfer from the host to the activator [24-26], the different thermal quenching of two emitters [16,18,27], the synergistic effect between defect centers and luminescence centers with different lattice site occupation [17, 28], or the interplay of defect levels and Pr^{3+}emission centers [29], visible color-tunable emission has been

detected with the increase of temperature.

The previous studies reveal that dynamic multicolor afterglow phosphors are associated with the existence of multiple luminescence centers and traps. To obtain temperature-dependent dynamic color-tunable inorganic phosphor-based materials, selecting the suitable host and activators is necessary [30-32]. A suitable matrix should possess multiple lattice sites to provide flexible site choices for doped active ions [33]. Doping with multiple ions is a classical method to introduce multiple luminescence centers, but energy loss is an unavoidable problem due to the existence of energy transfer [33]. So it's still a great challenge to select suitable substrates and dopants to achieve the dynamic color-tunable feature with only single-ion doping [26].

$Ca_3Ga_4O_9$ as one of gallates with multi cation sites has attracted considerable attention recently, with its defects such as gallium vacancies and oxygen vacancies acting as traps [34]. Trivalent Bi^{3+} dopant ions can be used to replace divalent Ca^{2+} ions in $Ca_3Ga_4O_9$: Bi^{3+} phosphors. Due to the charge imbalance between Ca^{2+} and Bi^{3+}, the incorporation of Bi^{3+} into $Ca_3Ga_4O_9$ creates $Bi_{Ca}^{\cdot}$ and V_{Ca}'' defects [35], and further increases the probability of non-radiative transitions [36]. Alkali metal ions such as Li^+, Na^+, and K^+ have frequently been employed to improve the emission intensity through charge compensation and by affecting the local site symmetry [36-39].

In our previous work, the $Ca_{2.95}Ga_4O_9$: 5 mol% Bi^{3+} sample showed the strongest thermoluminescence intensity. Therefore, in the present work, we propose a strategy to achieve temperature-dependent dynamic color-tunable luminescence by incorporating certain amounts of alkali metal ions into $Ca_{2.95}Ga_4O_9$: 5 mol% Bi^{3+}. Impressively, alkali metal ions not only improve the emission intensity but also change the trap distribution, providing remarkable dynamic color-tunable luminescence visually. These results offer a strategy for developing new multifunctional optical materials.

2. Experimental

$Ca_{2.95}Ga_4O_9$: 5 mol% Bi^{3+}, $Ca_{2.90}Ga_4O_9$: 5 mol% Bi^{3+}, 5 mol% A^+ (A=Li^+, Na^+, K^+) and $Ca_{2.95-x}Ga_4O_9$: 5 mol% Bi^{3+}, x mol% Na^+ (x=1, 3, 5, 7) phosphors were synthesized via the traditional solid-state method. Stoichiometric amounts of raw materials, including $CaCO_3$, Ga_2O_3, Bi_2O_3, Li_2CO_3, Na_2CO_3, K_2CO_3 and an appropriate amount

of ethanol were well mixed by grounding in an agate mortar for 30 mins. The homogeneous powder was put into an alumina crucible and transferred into a muffle furnace and sintered at 1210 ℃ for 10 h with a heating rate of 5 ℃/min in air or N_2/H_2 reduction atmosphere. Finally, after cooling down naturally to RT, the samples were ground again for later use.

The crystalline purity of all samples was checked by X-ray diffraction with Cu K α radiation (λ = 1.5406 Å). The Rietveld refinement was implemented by Fullprof software. Room temperature photoluminescence excitation (PLE) spectra, photoluminescence emission (PL) spectra were performed using an Edinburgh FS920 (Edinburgh Instruments Ltd, Livingston, UK) fluorescence spectrometer, equipped with a monochromated 450 W xenon arc lamp as excitation source. The reflectance spectra was measured using a PerkinElmer Lambda 1050 UV-vis-NIR spectrophotometer equipped with a Spectralon-coated integrating sphere with PMT (photomultiplier) and InGaAs detectors. The thermoluminescence (TL) spectra of the samples were collected by using a TOSL-3DS spectrometer. The temperature range was from 40 ℃ to 400 ℃ and the heating rate was 3 ℃ /s. The excitation sources of TL used in this work was 254 nm UV light. The decay times were collected using an EKSPLA NT340 series tunable laser as an excitation source in combination with an Andor intensified CCD. A small home-built vacuum chamber with a well-characterized cooling and heating stage was used for temperature-dependent PL measurements, a Linkam THMS600 temperature-controlled stage and fiber-based detection setup were used, the emission spectra were recorded by using Avantes. The excitation source were 280 nm or 340 nm xenon lamp. A long-pass filter with a cutoff wavelength of 320 nm and 380 nm were used to protect the detector from overexposure while exciting with the xenon lamp. Persistent luminescence decay profiles were collected using a ProEM1600EMCCD camera (Princeton Instruments) equipped with an Acton SP2300 monochromator after the samples were excited for 5 mins by white light.

3. Results and Discussions

The XRD patterns of $Ca_{2.95}Ga_4O_9$: 5 mol%Bi^{3+} and $Ca_{2.90}Ga_4O_9$: 5 mol% Bi^{3+}, 5 mol% A^+ (A^+ =Li^+, Na^+, K^+) phosphors are presented in Fig. 1(a). The main diffraction

patterns fit well with the standard PDF card no.83-1477 of $Ca_3Ga_4O_9$, which belongs to the orthorhombic system with the space group Cmm2. This indicates that the low concentration of metal ions added to the samples as charge compensators didn't lead to the change in the crystalline phase structure of the samples. In the $Ca_3Ga_4O_9$ structure, Ca^{2+} ions are distributed over two different sites, whose surroundings are sixfold and eightfold, whereas the Ga^{3+} ions occupy a fourfold coordination site [40,41], as shown in Fig. 1(b). Since the radius of Bi^{3+} (r=1.03 Å and 1.17 Å, CN = 6 and 8) is close to Ca^{2+} (r=1.00 Å and 1.12 Å, CN = 6 and 8) in $Ca_{2.95}Ga_4O_9$: 5 mol% Bi^{3+} phosphors [34,42], Bi^{3+} ions are supposed to exist in each of Ca^{2+} sites, but its occupancy rate can differ [35,43]. However, it would be difficult to maintain charge balance for a trivalent Bi^{3+} substituting a divalent Ca^{2+} ($Bi^{3+}\rightarrow Ca^{2+}$), which requires charge compensation to maintain the electrical neutrality of the system [44]. Therefore, monovalent cations such as Li^+, Na^+, and K^+ are doped to the $Ca_{2.95}Ga_4O_9$: 5 mol% Bi^{3+} phosphor. The Rietveld structure refinement results of $Ca_{2.90}Ga_4O_9$: 5 mol% Bi^{3+}, 5 mol% A^+ (A^+ =Li^+, Na^+, K^+) are presented in Fig. S1.

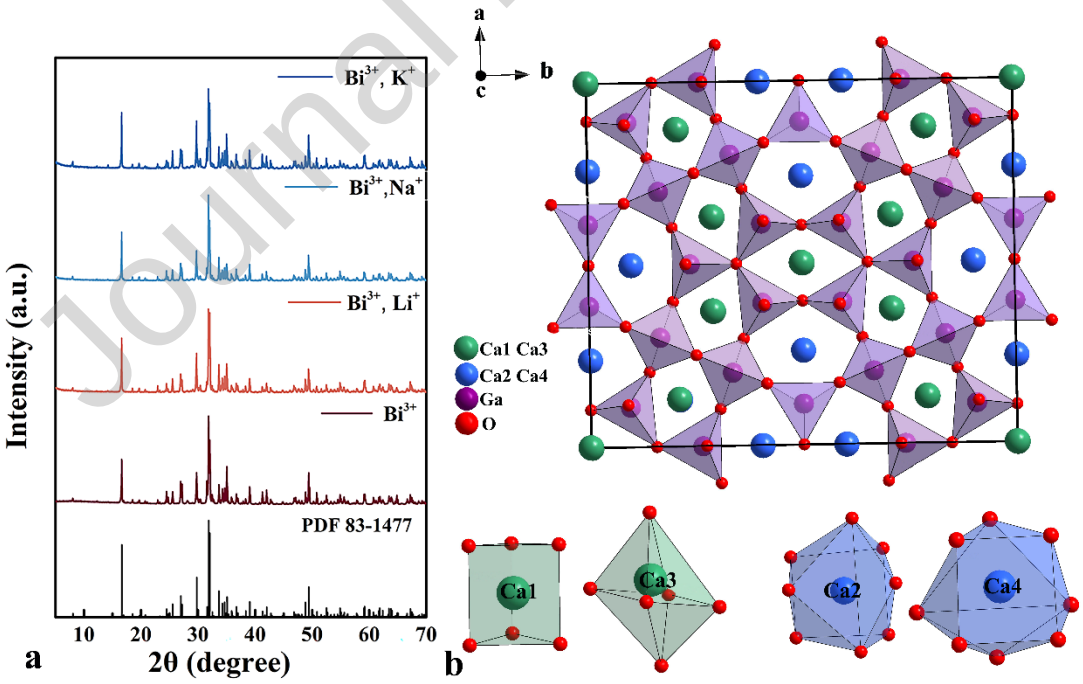

Fig. 1. a) XRD patterns of $Ca_{2.95}Ga_4O_9$: 5 mol%$Bi^{3+}$and $Ca_{2.90}Ga_4O_9$: 5 mol% Bi^{3+}, 5 mol% A^+ (A^+ =Li^+, Na^+, K^+) samples; b) the crystal structure of the $Ca_3Ga_4O_9$ host and the coordination environment of the Ca^{2+} ions.

The diffuse reflectance spectra of $Ca_3Ga_4O_9$ is shown in Fig. S2. $Ca_3Ga_4O_9$ shows

high reflection in the range of 300 nm- 800 nm, and then exhibits obvious energy absorption in the wavelength range of 200 nm-300 nm, ascribed to the host lattice absorption. The optical band gap was evaluated approximately to be 4.36 eV according to Kubelka-Munk theory [45,46].

The PLE and PL spectra of the $Ca_3Ga_4O_9$ are shown in Fig. 2(a), a blue broad band centered at 455 nm monitored at 258 nm is observed which is caused by the $^4T_2$-$^4A_2$ transition of electrons in d orbits of Ga^{3+}[34]. The excitation spectra of $Ca_{2.95}Ga_4O_9$: 5 mol% Bi^{3+} which are monitored at emission wavelength 578 nm (Em1) and 494 nm (Em2), and the emission spectra which are monitored at excitation wavelength 282 nm and 340 nm are shown in Fig. 2(b). It indicates that there are two emission centers of Bi^{3+} ions. Considering the energy levels of Bi^{3+} and the distinct crystallographic sites of Ca^{2+}, these two bands are attributed to the $^3P_1$–$^1S_0$ transition of Bi^{3+} in different sites [47-49]. The Em1 with larger stokes shift could be caused by that Bi^{3+}in Ca2 and Ca4 with 8 oxygen ligands due to the Pseudo-Jahn–Teller effect. Em2 should be attributed from Bi^{3+} in Ca1 and Ca3 sites with shorter Ca–O distances [48].

The emission band and excitation spectra of $Ca_{2.90}Ga_4O_9$: 5 mol% Bi^{3+}, 5 mol% A^+ (A^+=Li^+, Na^+, K^+) are shown in Fig. S3, which shows similar peak position with $Ca_{2.95}Ga_4O_9$: 5 mol% Bi^{3+}. But the addition of A^+ alkali (A^+=Li^+, Na^+, K^+) metal ions significantly change the intensity of emission. From the emission1 and emission2 intensity profile as shown in Fig. 2(c), it was noted that the PL intensity increased huge with co-doping of alkali metals. It is because that the Li^+, Na^+, and K^+ ions act as the charge compensators and fluxes, thereby maintaining the charge balance generated by the Bi^{3+} ions substituted in the Ca^{2+} sites and improving the crystallinity of samples [50,51]. Therefore the intensity of the emission increased. The gain of emission intensity upon co-doping is beneficial for emission 2 (the short wavelength component).

Among all samples, $Ca_{2.90}Ga_4O_9$: 5 mol% Bi^{3+}, 5 mol% Na^+ phosphor shows the strongest emission intensity. Charge compensation is an effective means to enhance the intensity of luminescent centers. It is not enough to consider it from the perspective of charge balance alone, but also volume balance [52]. The ionic radius of lithium ion R_{Li^+} (r=0.76 Å, CN=6; r=0.92 Å,CN=8) is smaller than the radius of a sodium ion

R_{Ca}^{2+}(r=1.00 Å, CN = 6; r=1.12 Å ,CN=8). The ionic radius of alkali metals Na^+ and K^+ are R_{Na}^+ (r=1.02 Å,CN=6; r=1.16 Å,CN=8) and R_K^+ (r=1.38 Å,CN=6; r=1.51 Å,CN=8) [53]. Na^+ has a similar ionic radius (1.02 Å) to that of the Ca^{2+} ionic radius (1.00 Å). Therefore, the incorporation equal amounts of Na^+ will minimize lattice distortions, thus the compensation effect of Na^+ on the luminescence performance of the samples is the most obvious, as shown in Fig. S3. Besides, the smaller Li^+ can make the crystal structure shrink, which effectively reduces the non-radiative transition. The bigger K^+ might have much more flux effect during the sintering [54].

Turning to the influence of Li^+, Na^+ and K^+ on the fluorescence spectra, it is noticed that the ratio of the two peaks has changed. Compared with the $Ca_{2.95}Ga_4O_9$: 5 mol% Bi^{3+} phosphor, co-doped with alkali metals increased the ratio of Em2/Em1, as shown in Fig. 2(b), which proves that co-doping has more obvious effect on the Em2 emission band. It is because that the substitution of alkali metal ions for Ca^{2+} could make the sites of Ca1 and Ca3 more suitable for Bi^{3+} substitution [49,54].

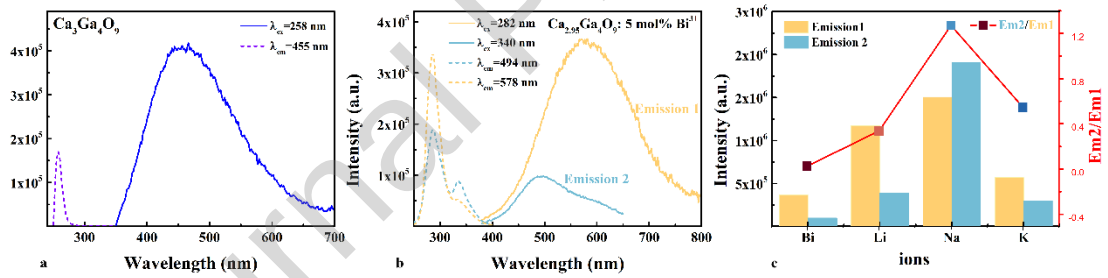

Fig. 2. PL and PLE spectra of (a) $Ca_3Ga_4O_9$ and (b) $Ca_{2.95}Ga_4O_9$:5 mol%Bi^{3+}; c) PL intensity of emission 1 monitored at 282 nm and emission 2 monitored at 340 nm, and the intensity ratio of Emission2/Emission1.

The decay curves of the two characteristic emissions in $Ca_{2.95}Ga_4O_9$: 5 mol% Bi^{3+} and $Ca_{2.90}Ga_4O_9$: 5 mol% Bi^{3+}, 5 mol% Na^+ could be well fitted to the double exponential formula in Eqs. (1) expressed as follows [55]:

$$I(t) = I_0 + A_1 \exp\left(\frac{t}{\tau_1}\right) + A_2 \exp\left(\frac{t}{\tau_2}\right) \quad (1)$$

where, I is the fluorescent intensity at time t, I_0 is the background or zero detector offset, τ_1 and τ_2 refer to the rapid and slow decay time of the exponential components, respectively, and the A parameters are the amplitudes of the two components. It can be calculated that the decay times (τ) of Em1 and Em2 emission are 2.08 μs, 1.45 μs of $Ca_{2.95}Ga_4O_9$: 5 mol% Bi^{3+}, and 6.17 μs, 0.64 μs of $Ca_{2.90}Ga_4O_9$: 5 mol% Bi^{3+}, 5 mol%

Na^+, which further validates the existence of two different kinds of emission centers, as shown in Fig.3.

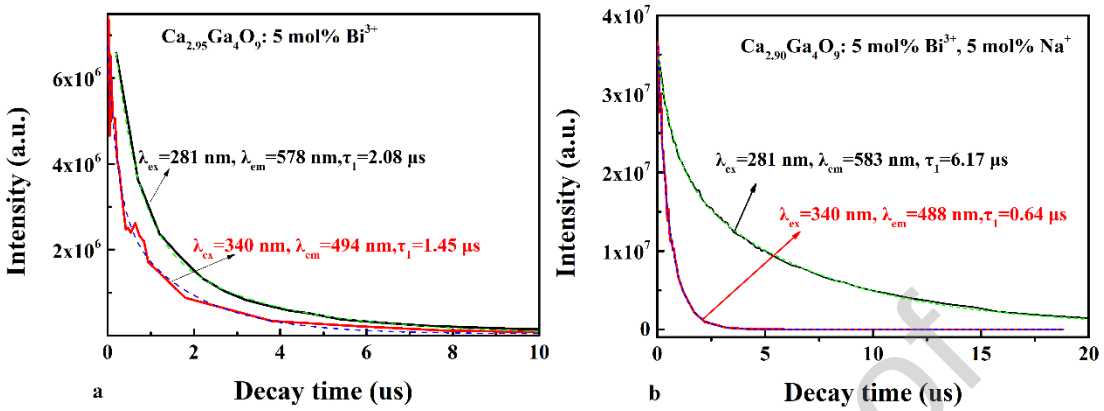

Fig. 3 Decay curves of (a) $Ca_{2.95}Ga_4O_9$: 5 mol% Bi^{3+} and (b) $Ca_{2.90}Ga_4O_9$: 5 mol% Bi^{3+}, 5 mol% Na^+.

The temperature-dependent dynamic color-tunable luminescence phenomenon of $Ca_{2.95}Ga_4O_9$: 5 mol%Bi^{3+} and $Ca_{2.90}Ga_4O_9$: 5 mol% Bi^{3+}, 5 mol% A^+ (A^+=Li^+, Na^+, K^+) samples are investigated with TL measurements after pre-illuminated by 254 nm UV light for 20 mins, as shown in Fig. 4 and S4. The wavelength of the thermoluminescence curve changes apparently with the variation of temperature in $Ca_{2.90}Ga_4O_9$: 5 mol% Bi^{3+}, 5 mol% A^+ (A^+=Li^+, Na^+, K^+) samples, especially the $Ca_{2.90}Ga_4O_9$: 5 mol% Bi^{3+}, 5 mol% Na^+ sample, as shown in Table S1. TL glow curves at different temperature of $Ca_{2.90}Ga_4O_9$: 5 mol% Bi^{3+}, 5 mol% Na^+ sample are shown in Fig.3(f). The relative intensity of two emission bands varies with the increase of the temperature. There is a red shift from 513 nm to 602 nm of the TL spectra. The same red-shift phenomenon can also be observed in $Ca_{2.90}Ga_4O_9$: 5 mol% Bi^{3+}, 5 mol% Li^+ and $Ca_{2.90}Ga_4O_9$: 5 mol% Bi^{3+}, 5 mol% K^+ samples, as shown in FigS4(c) and FigS4(f). Besides, the blue shift is also observed in $Ca_{2.90}Ga_4O_9$:5 mol%Bi^{3+}, 5 mol% K^+ sample at higher temperature.

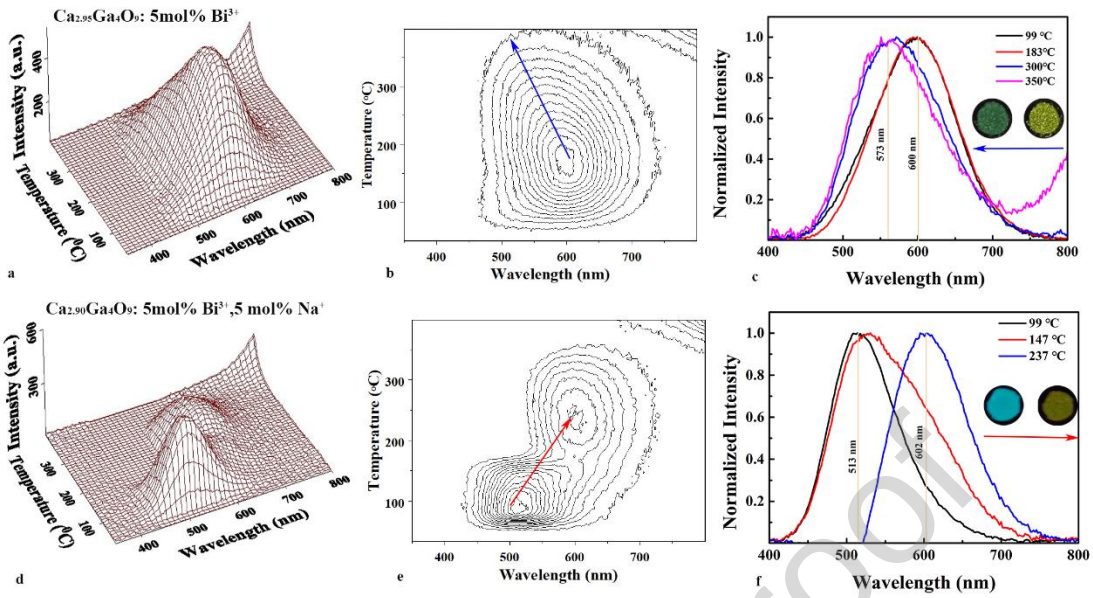

Fig. 4. a) 3D TL, b) contour map and (c) Normalized integrated TL emission spectral and photographs of $Ca_{2.95}Ga_4O_9$: 5 mol%Bi^{3+}; d) 3D TL, e) contour map and (f) Normalized integrated TL emission spectral and photographs of $Ca_{2.90}Ga_4O_9$:5 mol%Bi^{3+}, 5 mol% Na^+, the samples are pre-irradiated by a 254 nm UV lamp for 20 mins, the integration range is 30 °C before and after the indicated temperature.

The TL method is widely accepted as a powerful tool to reveal the properties of defect traps [16]. There is a successive trap distribution (40 ℃ – 400 ℃) for the material of $Ca_{2.95}Ga_4O_9$: 5 mol% Bi^{3+}.The wide temperature range recorded from 40 ℃-400 ℃ of the TL glow curve indicates that the phosphor has a broad distribution of traps [56]. It could be resolved as four TL peaks located at 75℃ (T_A), 125 ℃ (T_B), 225 ℃ (T_C) and 260 ℃ (T_D), respectively. The integrated TL glow curves (450 nm-700 nm) of samples $Ca_{2.90}Ga_4O_9$: 5 mol% Bi^{3+}, 5 mol% A^+ (A^+=Li^+, Na^+, K^+) are shown in Fig. 5. The charge compensator ions Li^+, Na^+ can enhance the intensity of shallow trap region (T_A, T_B), and reduce the intensity of the deep traps' region (T_C, T_D). There is also a successive trap distribution (40 ℃–400 ℃) for $Ca_{2.90}Ga_4O_9$: 5 mol% Bi^{3+}, 5 mol% K^+, which has fewer shallow traps and more deep traps compared with the $Ca_{2.95}Ga_4O_9$: 5 mol% Bi^{3+}.

To investigate the intrinsic defects in $Ca_3Ga_4O_9$, TL glow curves of undoped $Ca_3Ga_4O_9$ prepared under air, or a reducing atmosphere (N_2/H_2) are collected, as shown in Fig. S5. Additionally, it has been reported that more oxygen vacancies can be generated when samples are sintered under a poor oxygen atmosphere [57,58]. Hence,

$Ca_3Ga_4O_9$ sintered under a reducing atmosphere was tested, and the corresponding TL curves showed that the oxygen vacancies should be related to the TL glow peak T_A. Three Ca^{2+} ions would be substituted by two Bi^{3+} ions, $2Bi^{3+} + 3Ca^{2+} \rightarrow 2Bi_{Ca}^{\cdot} + V_{Ca}''$. Ca vacancy V_{Ca}'' and $Bi_{Ca}^{\cdot}$ would be created in $Ca_{2.95}Ga_4O_9$: 5 mol% Bi^{3+} phosphor [59]. When adding an appropriate amount of A^+ ions to the $Ca_3Ga_4O_9$ matrix, charge compensating ion A^+ can occupy the vacancies and enter the crystal of the $Ca_{2.95}Ga_4O_9$: 5 mol% Bi^{3+}phosphors. The positive charge of A^+ will neutralize the negative charge of V_{Ca}'' in the host and reduces the defects content of the phosphors [60-63], which may reduce the TL intensity in T_c and T_D region, as shown in Fig. 4. Since radius of Li^+ and Na^+ are smaller than K^+, they can be doped in the matrix more easily, which leads to obvious changes [60,64]. Besides, when a A^+ ion replaces the Ca^{2+} sites, A_{Ca}' and oxygen vacancies will be generated, which will form T_A traps [65]. Since the radius of K^+ is much bigger than Ca^{2+} in the host lattice, the doping would cause more lattice distortion. Thus T_C and T_D might come from the lattice distortion [66].

A further reality is that for dopants at say 5 mol % it implies there is on average one dopant per 20 host sites, hence they are always with ~ 3 sites of one another. Further, many dopant examples have indicated that they will pair or cluster [67]. In many systems the TL peak temperature suggest that dopants are paired with secondary ions (e.g. rare earth plus Li etc) and the peak values and temperatures scale with the size of the complex. This precisely a feature seen in Fig. 5and Fig. S4 in which Li, Na, add a lower temperature feature. This was a pattern noted in $CaSO_4$: RE TL [68,69]. Equally, the coupling between closely spaced dopant sites implies the possibility of a range of stabilities for TL, plus changing spectra. This is apparent from the higher temperature data of Fig. 5 and Fig. S4.

Whilst such complexity makes identification of sites virtually impossible it nevertheless is a powerful indicator of the opportunities to empirically adjust the changes in color of the TL.

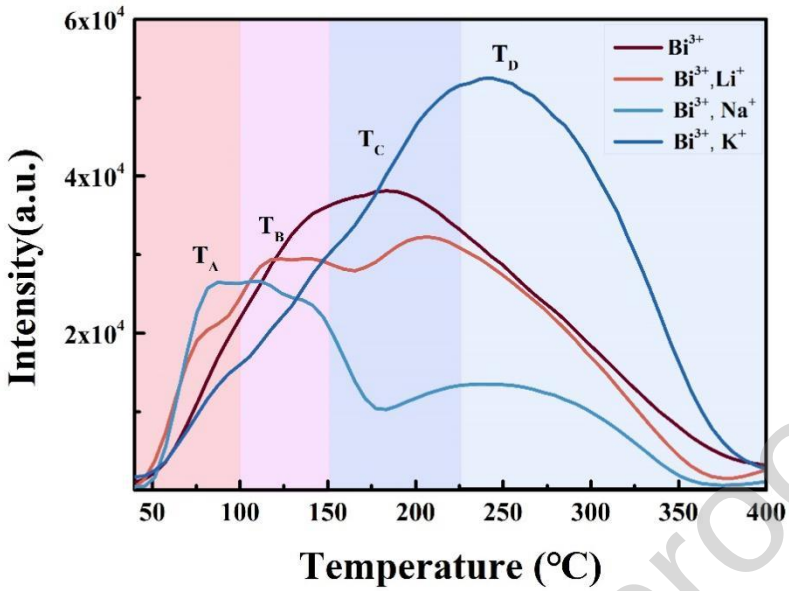

Fig. 5. TL glow curves of $Ca_{2.95}Ga_4O_9$:5 mol%$Bi^{3+}$and $Ca_{2.90}Ga_4O_9$: 5 mol% Bi^{3+}, 5 mol% A^+ (A^+ =Li^+, Na^+, K^+) samples.

It is quite uncommon to identify such a dynamic color-tunable feature during the thermoluminescence process [26]. To investigate the possibility of phase transitions during these temperature variations, the XRD patterns at different temperature are shown in Fig. S6. The results obviously reveal that there is no crystalline phase transition through the heating process but shows a thermal expansion of the lattice as seen from the shift of the diffraction peaks to smaller angles.

To investigate the possibility of thermal quenching of the two emission centers during temperature variations, the temperature-dependent PL spectra are shown in Fig. S7. As the temperature increases from -195 ℃ to 300 ℃, the PL intensity of these two emission bands show similar thermal response within the 40 ℃-300 ℃, so the color tunable properties are not related to thermal quenching [27]. Besides, the normalized temperature-dependent PL spectra of emission 1 shows a blue shift in the peak wavelength from 646 nm to 569 nm with the temperature increased from -195 ℃ to RT. As the temperature increases, the lattice will expand and the crystal field will weaken, resulting in blue shift of spectra [70].

The different phenomena between PL and TL at different temperature means that the red shift of the TL spectral with operating temperature is not due to the luminescent behavior of the luminescent center being affected by temperature, but the the energy

transfer process between traps and luminescence centers [71]. For thermoluminescence, the traps in the phosphor can store the energy under the excitation (i.e. 254 nm light), the stored energy is generally released and transferred to emission centers by heating after removing the excitation light. Due to the increase of temperature, the ratio of electrons returning to the two luminescence centers also changes. As for the origin of the two luminous centers, co-doping with alkali metal ions resulted in a significant enhancement of the Em2/Em1 intensity, whereas in TL it resulted in an enhancement of the relative intensity of the peak related to shallow trap/deep trap, which indicates that the TL and PL originate from the same luminescence centers. Therefore, the emission at 99 ℃ corresponds to the Em2 with the $^3P_1$-$^1S_0$ transition of Bi^{3+} at CaO_6 sites, while the emission monitored at 237 ℃ corresponds to the Em1 with $^3P_1$-$^1S_0$ transition of Bi^{3+} at CaO_8 sites. But the blue shift of $Ca_{2.95}Ga_4O_9$: 5 mol% Bi^{3+} and $Ca_{2.90}Ga_4O_9$: 5 mol% Bi^{3+}, 5 mol% K^+ at higher temperature may be due to the emission 1 effected by temperature.

The photos of $Ca_{2.90}Ga_4O_9$:5 mol%Bi^{3+}, 5 mol% A^+(A^+=Li^+, Na^+, K^+) powders on metal plates are obtained at certain temperature during heating after they are irradiated with 254 nm UV lamp for 30 minutes, as shown in Fig. 6. There is an obvious temperature-dependent color changeable from yellow to green in $Ca_{2.95}Ga_4O_9$:5 mol%Bi^{3+} phosphors. Co-doping with alkali metals increase the cyan emission at lower temperature, and the color change from cyan to yellow are detected in these samples. In addition, a color change from yellow to green at high temperature is also observed in the K-doped sample.

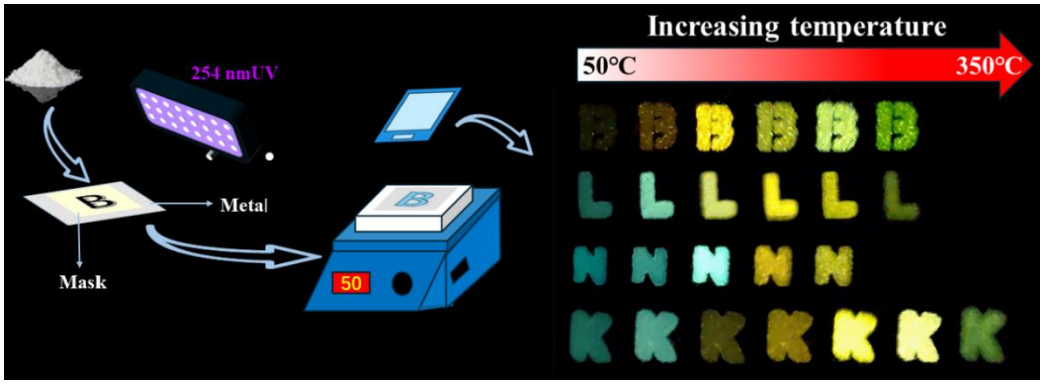

Fig. 6. Temperature-dependent color of $Ca_{2.95}Ga_4O_9$: 5 mol%Bi^{3+} and $Ca_{2.90}Ga_4O_9$: 5 mol% Bi^{3+},

5 mol% A^+(A^+=Li^+, Na^+, K^+) at different temperature after irradiation with 254 nm UV lamp for 30 mins.

Moreover, $Ca_{2.90}Ga_4O_9$: 5 mol% Bi^{3+}, 5 mol% Na^+ shows more pronounced cyan emission compared to yellow. According to the trap analysis above, there are more shallow traps in samples of $Ca_{2.90}Ga_4O_9$: 5 mol% Bi^{3+}, 5 mol% Na^+ and $Ca_{2.90}Ga_4O_9$: 5 mol% Bi^{3+}, 5 mol% Li^+ , which shows longer persistence decay time than $Ca_{2.90}Ga_4O_9$: 5 mol% Bi^{3+} which can be used in the field of long persistent luminescence, as shown in Fig. S8.

4. Conclusion

In summary, a traditional solid state reaction synthesis method is used for a series of $Ca_{2.95}Ga_4O_9$:5 mol%Bi^{3+} phosphors that were co-doped with the alkali A^+ (A^+ = Li^+, Na^+, K^+) metal ions to improve their dynamic color-tunable luminescence property. The charge compensators significantly increase the ratio of the emission intensity from the two emission centers (Em2/Em1). Among the charge compensators, Na^+ is the most effective ion in improving the PL properties of the $Ca_{2.95}Ga_4O_9$: 5 mol%Bi^{3+} phosphors, which is attributed to the similar ionic radii between Na^+ and Ca^{2+}. In addition, the charge compensation can fill the cation vacancies. The different Ca^{2+} sites and the difference with the ionic radius of alkali metal ions will have an impact on traps at different depths. Li^+ and Na^+ could increase the intensity of shallow traps, while K^+ increases the intensity of deep traps. Considering the interplay of different defects and two emission centers, co-doped samples show the obvious color variation from cyan to yellow with the temperature increase from 40 to 250 ℃. This work provides a strategy for the optimization of color-tunable persistent luminescence materials and their diversified applications.

Acknowledgements

The work has been supported by the China Scholarship Council (No.202306400093).

References

[1] P. Pei, P. DuanMu, B. Wang, X. Miao, C. Zhang, W. Liu, An advanced color tunable persistent luminescent $NaCa_2GeO_4F:Tb^{3+}$phosphor for multicolor anti-counterfeiting, Dalton Trans, 50 (2021) 3193-3200. https://doi.org/10.1039/d0dt04231e
[2] M. Martini, F. Meinardi, Thermally stimulated luminescence: new perspectives in the study of defects in solids, Riv. Nuovo Cim. 20 (1997) 1-71. https://doi.org/10.1007/BF02897907
[3] L. Yuan, Y. Jin, Y. Su, H. Wu, Y. Hu, S. Yang, Optically Stimulated Luminescence Phosphors: Principles, Applications, and Prospects, Laser Photonics Rev, 14 (2020) 2000123. https://doi.org/10.1002/lpor.202000123
[4] E.G. Yukihara, A.J.J. Bos, P. Bilski, S.W.S. McKeever, The quest for new thermoluminescence and optically stimulated luminescence materials: Needs, strategies and pitfalls, Radiat. Meas., 158 (2022) 106846. https://doi.org/10.1016/j.radmeas.2022.106846
[5] S. Tian, P. Feng, S. Ding, Y. Wang, Y. Wang, A color-tunable persistent luminescence material $LiTaO_3:Pr^{3+}$ for dynamic anti-counterfeiting, J. Alloys. Compd, 899 (2022) 163325. https://doi.org/10.1016/j.jallcom.2021.163325
[6] H. Guo, T. Wang, X. Zhu, H. Liu, L. Nie, L. Guo, T. Gu, X. Xu, X. Yu, Dynamic anti-counterfeiting and information encryption of $Sr_3Y_2Ge_3O_{12}$: Tb^{3+}, Er^{3+} phosphor via carriers filling and release processes, J Colloid Interface Sci, 640 (2023) 719-726. https://doi.org/10.1016/j.jcis.2023.02.158
[7] Y. Zhan, Y. Jin, H. Wu, L. Yuan, G. Ju, Y. Lv, Y. Hu, Cr^{3+}-doped $Mg_4Ga_4Ge_3O_{16}$ near-infrared phosphor membrane for optical information storage and recording, J. Alloys. Compd, 777 (2019) 991-1000. https://doi.org/10.1016/j.jallcom.2018.11.065
[8] L. Zhao, T. Liu, H. An, H. Wang, K. Lv, J. Huang, X. Li, J. Zhou, Design and characterization of Eu^{2+}-doped $Ba_4Si_6O_{16}$ photostimulated phosphor for optical information storage, J. Lumin, 227 (2020) 117556. https://doi.org/10.1016/j.jlumin.2020.117556
[9] M. Sen, R. Shukla, N. Pathak, K. Bhattacharyya, V. Sathian, P. Chaudhury, M.S. Kulkarni, A.K. Tyagi, Development of $LiMgBO_3:Tb^{3+}$ as a new generation material for thermoluminescence based personnel neutron dosimetry, Mater Adv, 2 (2021) 3405-3419. https://doi.org/10.1039/d0ma00737d
[10] P. Seth, A. Jain, L. Goswami, G. Gupta, S. Aggarwal, Defect Induced MgO: Li, Sm nanophosphor as a new highly sensitive material for thermoluminescence dosimetry, J. Alloys. Compd, 965 (2023) 171329. https://doi.org/10.1016/j.jallcom.2023.171329
[11] A. Vidya Saraswathi, N.S. Prabhu, K. Naregundi, M.I. Sayyed, M.S. Murari, A.H. Almuqrin, S.D. Kamath, Thermoluminescence investigations of $Ca_2Al_2SiO_7$: Dy^{3+} phosphor for gamma dosimetry applications, Mater. Chem. Phys, 281 (2022) 125872. https://doi.org/10.1016/j.matchemphys.2022.125872
[12] H. Jin, Y. Zhao, Y. Wang, L. Xi, L. Yin, Y. Ma, P.D. Townsend, Improved thermoluminescence response of terbium doped magnesium orthosilicate by co-doping with sodium ions, Opt. Mater, 98 (2019) 109448. https://doi.org/10.1016/j.optmat.2019.109448

[13] Z. Yang, J. Hu, D. Van der Heggen, A. Feng, H. Hu, H. Vrielinck, P.F. Smet, D. Poelman, Realizing Simultaneous X-Ray Imaging and Dosimetry Using Phosphor-Based Detectors with High Memory Stability and Convenient Readout Process, Adv. Func. Mater, 32 (2022) 2201684. https://doi.org/10.1002/adfm.202201684
[14] Z. Yang, J. Hu, D. Van der Heggen, M. Jiao, A. Feng, H. Vrielinck, P.F. Smet, D. Poelman, A Versatile Photochromic Dosimeter Enabling Detection of X-Ray, Ultraviolet, and Visible Photons, Laser & Photonics Rev, 17 (2023) 2200809. https://doi.org/10.1002/lpor.202200809
[15] Z. Yang, J.J. Joos, J. Hu, D. Van der Heggen, T. Pier, M. Delaey, H. Vrielinck, T. Jüstel, P.F. Smet, D. Poelman, Personal Solar UV Monitoring based on Photoinduced Electron Transfers in Luminescent Materials, Adv. Opt. Mater, 11 (2023) 2300733. https://doi.org/10.1002/adom.202300733
[16] J. Zhang, Z. Wang, X. Huo, Y. Wang, P. Li, Multimodal dynamic color-tunable persistent luminescent phosphor $Ca_3Al_2Ge_3O_{12}$:Mn^{2+}, Cr^{3+} for anti-counterfeiting and industrial inspection, Inorg. Chem. Front., 9 (2022) 6517-6526. https://doi.org/10.1039/d2qi02041f
[17] Y. Tang, M.D.Z. Zhou, J. Wang, Q. Liu, A multicolor-emitted phosphor for temperature sensing and multimode dynamic anti-counterfeiting, J. Am. Ceram. Soc, 105 (2022) 6241-6251. https://doi.org/10.1111/jace.18587
[18] Z. Zuo, Y. Peng, J. Li, X. Wang, Z. Liu, Y. Chen, Thermal-responsive dynamic color-tunable persistent luminescence from green to deep red for advanced anti-counterfeiting, Chem. Eng. J, 446 (2022) 136976. https://doi.org/10.1016/j.cej.2022.136976
[19] M. Chen, Z. Xia, M.S. Molokeev, C.C. Lin, C. Su, Y.-C. Chuang, Q. Liu, Probing Eu^{2+} Luminescence from Different Crystallographic Sites in $Ca_{10}M(PO_4)_7$: Eu^{2+} (M = Li, Na, and K) with β-$Ca_3(PO_4)_2$-Type Structure, Chem Mater, 29 (2017) 7563-7570. https://doi.org/10.1021/acs.chemmater.7b02724
[20] Z. Wang, W. Wang, H. Zhou, J. Zhang, S. Peng, Z. Zhao, Y. Wang, Superlong and Color-Tunable Red Persistent Luminescence and Photostimulated Luminescence Properties of $NaCa_2GeO_4F$: Mn^{2+}, Yb^{3+} Phosphor, Inorg Chem, 55 (2016) 12822-12831. https://doi.org/10.1021/acs.inorgchem.6b02136
[21] X. Tang, D. Jin, J. Zhao, M. Jin, Color tuning of Bi^{3+}-doped double-perovskite $Ba_2(Gd_{1-x}, Lu_x)$ NbO_6 ($0 \leq x \leq 0.6$) solid solution compounds via crystal field modulation for white LEDs, RSC Adv, 10 (2020) 25500-25508. https://doi.org/10.1039/d0ra03793a
[22] Z. An, W. Liu, Y. Song, X. Zhang, R. Dong, X. Zhou, K. Zheng, Y. Sheng, Z. Shi, H. Zou, Color-tunable Eu^{2+}, Eu^{3+} co-doped $Ca_{20}Al_{26}Mg_3Si_3O_{68}$ phosphor for W-LEDs, J. Mater Chem C, 7 (2019) 6978-6985. https://doi.org/10.1039/C9TC01974J.
[23] Y. Fan, X. Jin, M. Wang, Y. Gu, J. Zhou, J. Zhang, Z. Wang, Multimode dynamic photoluminescent anticounterfeiting and encryption based on a dynamic photoluminescent material, Chem. Eng. J, 393 (2020) 124799. https://doi.org/10.1016/j.cej.2020.124799
[24] X. Zhang, H. Guo, Q. Shi, C. Cui, Y. Cui, P. Huang, L. Wang, The color-tunable persistent luminescence of Pr^{3+}-activated $Ca_2Sb_2O_7$ with double anti-counterfeiting

potentiality, Ceram. Int, 48 (2022) 36201-36209. https://doi.org/10.1016/j.ceramint.2022.08.177
[25] Z. Wei, W. Chen, Z. Wang, N. Li, P. Zhang, M. Zhang, L. Zhao, Q. Qiang, High-temperature persistent luminescence and visual dual-emitting optical temperature sensing in self-activated $CaNb_2O_6$: Tb^{3+}phosphor, J. Am. Ceram. Soc., 104 (2020) 1750-1759. https://doi.org/10.1111/JACE.17579
[26] J. Du, S. Lyu, P. Wang, T. Wang, H. Lin, Multimode-Responsive Luminescence Smart Platform by Single-Sm^{3+}-Doped Phosphors, Adv. Opt. Mater., 11 (2023) 2300359. https://doi.org/10.1002/adom.202300359
[27] Y. Tang, Y. Cai, K. Dou, J. Chang, W. Li, S. Wang, M. Sun, B. Huang, X. Liu, J. Qiu, L. Zhou, M. Wu, J.C. Zhang, Dynamic multicolor emissions of multimodal phosphors by Mn2+ trace doping in self-activated $CaGa_4O_7$, Nat Commun, 15 (2024) 3209. https://doi.org/10.1038/s41467-024-47431-0
[28] J. Wu, L. Zhao, W. Chen, Y. Yang, Y. Wang, X. Xu, Dynamic readout of optical information based on the color-tunable emitting electron-trapping material $BaAl_{12}O_{19}$:Eu^{2+} toward high security level optical data storage and anticounterfeiting, Inorg. Chem. Front., 10 (2023) 2474-2483. https://doi.org/10.1039/d3qi00160a
[29] X. Zhou, L. Ning, J. Qiao, Y. Zhao, P. Xiong, Z. Xia, Interplay of defect levels and rare earth emission centers in multimode luminescent phosphors, Nat Commun, 13 (2022) 7589. https://doi.org/10.1038/s41467-022-35366-3
[30] M. Shang, C. Li, J. Lin, How to produce white light in a single-phase host? Chem. Soc. Rev., 43 (2014) 1372-1386. https://doi.org/10.1039/c3cs60314h
[31] Z. Long, Y. Wen, J. Qiu, J. Wang, D. Zhou, C. Zhu, J.a. Lai, X. Xu, X. Yu, Q. Wang, Crystal structure insight aided design of $SrGa_2Si_2O_8$:Mn^{2+} with multi-band and thermally stable emission for high-power LED applications, Chem. Eng. J, 375 (2019) 122016. https://doi.org/10.1016/j.cej.2019.122016
[32] A. Bessière, S.K. Sharma, N. Basavaraju, K.R. Priolkar, L. Binet, B. Viana, A.J.J. Bos, T. Maldiney, C. Richard, D. Scherman, D. Gourier, Storage of Visible Light for Long-Lasting Phosphorescence in Chromium-Doped Zinc Gallate, Chem. Mater., 26 (2014) 1365-1373. https://doi.org/10.1021/cm403050q
[33] X. Li, P. Li, C. Liu, L. Zhang, D. Dai, Z. Xing, Z. Yang, Z. Wang, Tuning the luminescence of $Ca_9La(PO_4)_7$: Eu^{2+}via artificially inducing potential luminescence centers, J. Mater. Chem. C, 7 (2019) 14601-14611. https://doi.org/10.1039/c9tc04828f
[34] Z. Long, Y. Wen, J. Zhou, J. Qiu, H. Wu, X. Xu, X. Yu, D. Zhou, J. Yu, Q. Wang, No-Interference Reading for Optical Information Storage and Ultra-Multiple Anti-Counterfeiting Applications by Designing Targeted Recombination in Charge Carrier Trapping Phosphors, Adv. Opt. Mater., 7 (2019) 1900006. https://doi.org/10.1002/adom.201900006
[35] L. Yin, Y. Wang, L. Pan, S. Qiao, M. Zhang, Y. Li, P.D. Townsend, Enhancing the optical information storage performance of $Ca_3Ga_4O_9$: Bi^{3+} by co-doping with Zn^{2+} ions, Opt. Mater, 125 (2022) 112129. https://doi.org/10.1016/j.optmat.2022.112129
[36] J. Wu, X. Pan, L. Wen, L. Luo, Q. Zhou, Design a rare-earth free broadband NIR phosphor and improve the photoluminescence intensity by alkali charge compensation, Mater Today Commun, 30 (2022) 102997.

https://doi.org/10.1016/j.mtcomm.2021.102997
[37] C.M. Nandanwar, A.N. Yerpude, N.S. Kokode, S.J. Dhoble, Effect of charge compensators A^+ (A^+ = Li, Na and K) on photoluminescence properties of $Ba_2Ca(PO_4)_2$: Eu^{3+} phosphor for solid state lighting, J. Mater. Sci. Mater. Electron., 34 (2023) 1464. https://doi.org/10.1007/s10854-023-10889-7
[38] X. Yu, X. Xu, C. Zhou, J. Tang, X. Peng, S. Yang, Synthesis and luminescent properties of $SrZnO_2$:Eu^{3+}, M^+ (M=Li, Na, K) phosphor, Mater. Res. Bull., 41 (2006) 1578-1583. https://doi.org/10.1016/j.materresbull.2006.02.001
[39] F. Yang, Y. Liang, M. Liu, X. Li, N. Wang, Z. Xia, Enhanced red-emitting by charge compensation in Eu^{3+}-activated Ca_2BO_3Cl phosphors, Ceram Int, 38 (2012) 6197-6201. https://doi.org/10.1016/j.ceramint.2012.04.071
[40] Y. Yasui, E. Niwa, M. Matsui, K. Fujii, M. Yashima, Discovery of a Rare-Earth-Free Oxide-Ion Conductor $Ca_3Ga_4O_9$ by Screening through Bond Valence-Based Energy Calculations, Synthesis, and Characterization of Structural and Transport Properties, Inorg Chem, 58 (2019) 9460-9468.
https://doi.org/10.1021/acs.inorgchem.9b01300
[41] A.R. Schulze, H. Müller-Buschbaum, Über Erdalkalimetalloxogallate. VIII Synthese und Aufbau eines neuen Calciumoxogallats: $Ca_3Ga_4O_9$. Monatshefte für Chemie 112 (1981) 149-156. https://doi.org/10.1007/BF00911081
[42] R.D. Shannon, Revised Effective Ionic Radii and Systematic Studies of Interatomie Distances in Halides and Chalcogenides, Acta Cryst., 32 (1976) 751-767. https://doi.org/10.1107/S0567739476001551
[43] D. Liu, X. Yun, G. Li, P. Dang, M.S. Molokeev, H. Lian, M. Shang, J. Lin, Enhanced Cyan Emission and Optical Tuning of $Ca_3Ga_4O_9$:$Bi^{3+}$for High-Quality Full-Spectrum White Light-Emitting Diodes, Adv. Opt. Mater, 8 (2020) 2001037. https://doi.org/10.1002/adom.202001037
[44] M. Puchalska, E. Zych, P. Bolek, Luminescences of Bi^{3+} and Bi^{2+} ions in Bi-doped $CaAl_4O_7$ phosphor powders obtained via modified Pechini citrate process, J. Alloys. Compd, 806 (2019) 798-805. https://doi.org/10.1016/j.jallcom.2019.07.307
[45] H. Li, R. Zhao, Y. Jia, W. Sun, J. Fu, L. Jiang, S. Zhang, R. Pang, C. Li, $Sr_{1.7}Zn_{0.3}CeO_4$: Eu^{3+} novel red-emitting phosphors: synthesis and photoluminescence properties, ACS Appl. Mater. Interfaces, 6 (2014) 3163-3169.
https://doi.org/10.1021/am4041493
[46] X. Li, P. Li, Z. Wang, S. Liu, Q. Bao, X. Meng, K. Qiu, Y. Li, Z. Li, Z. Yang, Color-Tunable Luminescence Properties of Bi^{3+} in $Ca_5(BO_3)_3F$ via Changing Site Occupation and Energy Transfer, Chem. Mater., 29 (2017) 8792-8803.
https://doi.org/10.1021/acs.chemmater.7b03151
[47] W. Sun, R. Pang, H. Li, D. Li, L. Jiang, S. Zhang, J. Fu, C. Li, Investigation of a novel color tunable long afterglow phosphor $KGaGeO_4$:Bi^{3+}: luminescence properties and mechanism, J. Mater. Chem. C, 5 (2017) 1346-1355.
https://doi.org/10.1039/C6TC04012H
[48] H. Ju, J. Liu, B. Wang, X. Tao, Y. Ma, S. Xu, Bi^{3+}-doped $Sr_3Al_2O_6$: An unusual color-tunable phosphor for solid state lighting, Ceram. Int., 39 (2013) 857-860.
http://dx.doi.org/10.1016/j.ceramint.2012.05.106

[49] H. Li, R. Pang, Y. Luo, H. Wu, S. Zhang, L. Jiang, D. Li, C. Li, H. Zhang, Structural Micromodulation on Bi^{3+}-Doped $Ba_2Ga_2GeO_7$ Phosphor with Considerable Tunability of the Defect-Oriented Optical Properties, ACS Appl. Electron. Mater., 1 (2019) 229-237. https://doi.org/10.1021/acsaelm.8b00072
[50] G.W. Jung, K. Park, Effect of monovalent charge compensators on the photoluminescence properties of $Ca_3(PO_4)_2$: Tb^{3+}, A^+ (A = Li, Na, K) phosphors, J. Mater Sci Technol, 82 (2021) 187-196. https://doi.org/10.1016/j.jmst.2020.11.065
[51] M. Jayachandiran, S.M.M. Kennedy, Investigation of alkali metals (A^+ = K, Na, Li) co-doped with samarium ions in the eulytite-type phosphate based phosphors for the enhancement of luminescence properties, J. Lumin., 219 (2020) 116951. https://doi.org/10.1016/j.jlumin.2019.116951
[52] I. Billard, Lanthanide and actinide solution chemistry as studied by time-resolved emission spectroscopy, in, 2003, pp. 465-514.
[53] F. Zhao, Z. Song, Q. Liu, Color-Tunable Persistent Luminescence of $Ca_{10}M(PO_4)_7$: Eu^{2+} (M = Li, Na, and K) with a beta-$Ca_3(PO_4)_2$-Type Structure, Inorg. Chem, 60 (2021) 3952-3960. https://doi.org/10.1021/acs.inorgchem.0c03773
[54] L. Ruan, Z. Zhou, Y. Hu, R. Peng, X. Chen, M. Cheng, Z. Zhou, M. Xia, A narrow-band blue emitting phosphor by co-doping Bi^{3+} and alkali metal ions (Li^+, Na^+ and K^+) with dual luminescence center, J. Rare Earths, (2024) https://doi.org/10.1016/j.jre.2024.03.016.
[55] K. Li, J. Fan, M. Shang, H. Lian, J. Lin, $Sr_2Y_8(SiO_4)_6O_2$: Bi^{3+}/Eu^{3+}: a single-component white-emitting phosphor via energy transfer for UV w-LEDs, J. Mater. Chem. C, 3 (2015) 9989-9998. https://doi.org/10.1039/c5tc01993a
[56] H. Li, H. Wu, R. Pang, G. Liu, S. Zhang, L. Jiang, D. Li, C. Li, J. Feng, H. Zhang, Investigation on the photoluminescence and thermoluminescence of $BaGa_2O_4$:Bi^{3+} at extremely low temperatures, J. Mater. Chem. C, 9 (2021) 1786-1793. https://doi.org/10.1039/d0tc05122e
[57] T. Matsuzawa, Y. Aoki, N. Takeuchi, Y. Murayama, A New Long Phosphorescent Phosphor with High Brightness, $SrAl_2O_4$: Eu^{2+}, Dy^{3+} J. Electrochem. Soc., 143 (2019) 2670-2673. https://doi.org/10.1149/1.1837067
[58] I. Norrbo, J.M. Carvalho, P. Laukkanen, J. Mäkelä, F. Mamedov, M. Peurla, H. Helminen, S. Pihlasalo, H. Härmä, J. Sinkkonen, M. Lastusaari, Lanthanide and Heavy Metal Free Long White Persistent Luminescence from Ti Doped Li–Hackmanite: A Versatile, Low-Cost Material, Adv. Func. Mater, 27 (2017) 1606547. https://doi.org/10.1002/adfm.201606547
[59] Z. Long, J. Zhou, J. Qiu, Q. Wang, D. Zhou, X. Xu, X. Yu, H. Wu, Z. Li, Thermally stable photoluminescence and long persistent luminescence of $Ca_3Ga_4O_9$: Tb^{3+}/Zn^{2+}, J. Rare Earths, 36 (2018) 675-679. https://doi.org/10.1016/j.jre.2017.11.016
[60] I.P. Sahu, Effect of charge compensator ions (R^+ = Li^+, Na^+ and K^+) on $Sr_2MgSi_2O_7$:Dy^{3+} phosphors by solid-state reaction method, Appl. Phys. A, 122 (2016) 6721. https://doi.org/10.1007/s00339-016-0379-y
[61] D.-D. Xua, W. Zhou, Z. Zhang, S.-J. Li, X.-R. Wang, Improved photoluminescence by charge compensation in Dy^{3+} doped $Sr_4Ca(PO_4)_2SiO_4$

phosphor, Opt. Mater, 89 (2019) 197-202.
https://doi.org/10.1016/j.optmat.2019.01.041
[62] I.P. Sahu, D.P. Bisen, N. Brahme, R.K. Tamrakar, G. Banjare, P. Dewangan, Luminescent properties of R^+ doped $Sr_2MgSi_2O_7:Eu^{3+}$ ($R^+ = Li^+$, Na^+ and K^+) orange–red emitting phosphors, J. Mater. Sci. Mater. Electron., 27 (2016) 6721-6734.
https://doi.org/10.1007/s10854-016-4621-3
[63] S. Yao, L. Chen, Y. Huang, W. Li, Enhanced luminescence of $CaSb_2O_6:Bi^{3+}$ blue phosphors by efficient charge compensation, Mater Sci Semicond Process, 41 (2016) 265-269. https://doi.org/10.1016/j.mssp.2015.09.015
[64] G.R. Banjare, D.P. Bisen, N. Brahme, C. Belodhiya, P. Dewangan, E. Chandrawansi, I.P. Sahu, Thermoluminescence studies of Dy^{3+}-doped calcium barium orthosilicate codoped with Li^+ ion, J. Therm. Anal. Calorim, 139 (2019) 1577-1583.
https://doi.org/10.1007/s10973-019-08520-1
[65] G.-H. Li, P.-F. Wu, B. Ye, G.-M. Cai, Enhancement of Eu^{2+} photoluminescence behavior in $NaBaB_9O_{15}$ based on the K^+ doping, J. Lumin., 243 (2022) 118613.
https://doi.org/10.1016/j.jlumin.2021.118613
[66] H. Sun, Q. Zhu, J.-G. Li, Local charge regulation by doping Li^+ in $BaGa_2O_4:Bi^{3+}$ to generate multimode luminescence for advanced optical Morse code, Ceram. Int., 48 (2022) 9640-9650. https://doi.org/10.1016/j.ceramint.2021.12.163
[67] P.D. Townsend, Y. Wang, Improving interpretations of imperfections in insulating materials for current technologies, Opt. Mater X, 22 (2024) 100327.
https://doi.org/10.1016/j.omx.2024.100327
[68] S.W.S. McKeever, An overview of, and prospects for, new luminescent detectors, Radiat. Meas, 171 (2024) 107062. https://doi.org/10.1016/j.radmeas.2024.107062
[69] T Karali, A P Rowlands, P D Townsend, M. Prokic., J. Olivares, Spectral comparison of Dy, Tm and Dy/Tm in thermoluminescent dosimeters, J. Phys. D: Appl. Phys., 31 (1998) 754-765. https://doi.org/10.1088/0022-3727/31/6/025
[70] K. Chen, P. Gao, Z. Zhang, Y. Ma, Z. Luo, M.S. Molokeev, Z. Zhou, M. Xia, Zero-thermal-quenching broadband yellow-emitting Bi^{3+}-activated phosphors based on metal to metal charge transfer, J. Alloys. Compd, 986 (2024) 174112.
https://doi.org/10.1016/j.jallcom.2024.174112
[71] P. Zhang, W. Xie, Z. Wang, Z. Lin, X. Huang, Z. Ju, W. Liu, Time-dependent dynamic multicolor afterglow of simple $LiGa_5O_8:Eu^{3+}/Tb^{3+}$particles for advanced anticounterfeiting and encryption, Inorg. Chem. Front., 9 (2022) 4022-4029.
https://doi.org/ 10.1039/d2qi00836j

Graphical abstract

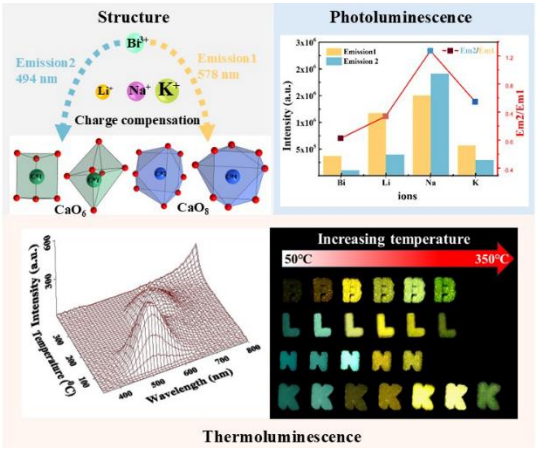

Declaration of interests

☒ The authors declare that they have no known competing financial interests or personal relationships that could have appeared to influence the work reported in this paper.

☐The authors declare the following financial interests/personal relationships which may be considered as potential competing interests:

Highlights:

- The Bi^{3+} and alkali metal ions co-doped $Ca_3Ga_4O_9$ phosphors have been synthesized.
- Co-doping can enhance the luminescence intensity of emission 2, especially for Na^+ ions.
- The dynamic color variation with the increase of temperature was achieved after co-doping.